



저작자표시-비영리-변경금지 2.0 대한민국

이용자는 아래의 조건을 따르는 경우에 한하여 자유롭게

- 이 저작물을 복제, 배포, 전송, 전시, 공연 및 방송할 수 있습니다.

다음과 같은 조건을 따라야 합니다:



저작자표시. 귀하는 원저작자를 표시하여야 합니다.



비영리. 귀하는 이 저작물을 영리 목적으로 이용할 수 없습니다.



변경금지. 귀하는 이 저작물을 개작, 변형 또는 가공할 수 없습니다.

- 귀하는, 이 저작물의 재이용이나 배포의 경우, 이 저작물에 적용된 이용허락조건을 명확하게 나타내어야 합니다.
- 저작권자로부터 별도의 허가를 받으면 이러한 조건들은 적용되지 않습니다.

저작권법에 따른 이용자의 권리는 위의 내용에 의하여 영향을 받지 않습니다.

이것은 [이용허락규약\(Legal Code\)](#)을 이해하기 쉽게 요약한 것입니다.

[Disclaimer](#)

공학석사학위논문

Discovery of *O*-methyltransferase for
site-specific methylation of Epigallocatechin
gallate (EGCG)

에피갈로카테킨 갈레이트(EGCG)의
위치특이적 메틸화를 위한 *O*-메틸전환효소의 발굴

2022 년 2 월

서울대학교 대학원

공과대학 협공과정 바이오엔지니어링

박 경 국

Discovery of O-methyltransferase for
site-specific methylation of Epigallocatechin
gallate (EGCG)

By

Gyeongguk park

Advisor: Professor Byung-Gee Kim, Ph.D.

Submitted in partial fulfillment of the requirement
for
the Master of Science in engineering degree

February 2022

Interdisciplinary Program for bioengineering
Seoul National University

Discovery of *O*-methyltransferase for site-specific
methylation of epigallocatechin gallate (EGCG)

에피갈로카테킨 갈레이트(EGCG)의 위치특이적
메틸화를 위한 *O*-메틸전환효소의 발굴

지도교수 김병기

이 논문을 공학석사 학위논문으로 제출함

2022년 2월

서울대학교 대학원

공과대학 협동과정 바이오엔지니어링

박 경 국

박경국의 공학석사 학위论문을 인준함

2022년 2월

위 원 장 _____ (인)

부위원장 _____ (인)

위 원 _____ (인)

Abstract

The (-)-Epigallocatechin-3-*o*-gallate (EGCG) in tea extract is the promising nutraceutical agent. Due to various health effects of EGCG, it is used as dietary supplements or therapeutic drugs. However, many studies reported the poor bioavailability of EGCG on oral administration, which hamper its application. The site-specific methylation modification to EGCG, especially 3'' hydroxyl group in D-ring, significantly enhanced its stability and bioavailability in human body. Therefore, the methylation modification is the way to make EGCG more orally active and potent nutraceutical agents in the market.

In this study, for the effective synthesis of the methylated EGCG, we adopted the enzymatic method with the S-adenosyl-L-methionine (SAM) dependent *o*-methyltransferase which carried out the methyl transfer reaction. Previously, our lab found out *o*-methyltransferases from *bacillus licheniformis* and *bacillus megaterium* which transfer methyl group to EGCG. *bm*OMT with low regioselectivity produced the multiple methylated EGCG. In contrast, *b*OMT had relatively high regioselectivity and produced 3''Me EGCG as the major product.

To improve the production of 3''Me EGCG, we conducted the site-directed mutagenesis based on PCR by using rational design. We engineered the *b*OMT which has high regioselectivity and confirmed that

the F163W mutant shows 2-fold increase of initial velocity. And we tried to seek the more active OMT by using bioinformatics tools, Subgrouping Automata and docking simulation. We found out the more active and regioselective bacterial OMTs from *thermolongibacillus altinseunsis* and *bacillus subtilis*. the catalytic activity of *ta*OMT and *bs*OMT was better than *b*OMT. The catalytic ratio (K_{cat}/K_m) of *ta*OMT for EGCG is at $17.4 \text{ M}^{-1} \text{ s}^{-1}$, about 2-fold higher than that of *b*OMT at $8.7 \text{ M}^{-1} \text{ s}^{-1}$. And the *bs*OMT is at $11.3 \text{ M}^{-1} \text{ s}^{-1}$, about 1.3-fold higher than *b*OMT.

Key Words: (-)-Epigallocatechin-gallate (EGCG), (-)-Epigallocatechin-3-*O*-(3-*O*-methyl)-gallate (3'-Me EGCG), SAM dependent *O*-methyltransferase, Enzyme engineering, virtual screening

Student Number: 2020-28874

Abbreviations:

*b*OMT: *bacillus licheniformis o*-methyltransferase

*bm*OMT: *bacillus megaterium o*-methyltransferase

*pc*OMT: *paenibacillus chondroitinus o*-methyltransferase

*hv*OMT: *heyndrickxia vini o*-methyltransferase

*ta*OMT: *thermolongibacillus altinseunsis o*-methyltransferase

*bs*OMT: *bacillus subtilis o*-methyltransferase

Contents

ABSTRACT.....	1
CONTENTS	4
LIST OF FIGURES	6
LIST OF TABLES.....	6
1. INTRODUCTION.....	10
2. MATERIALS AND METHODS.....	111
2.1.1. Chemicals and materials.....	11
2.1.2. Sequence alignments and Docking simulation	12
2.1.3. Site-directed mutagenesis.....	12
2.1.4. Expression and purification of the enzymes.....	156
2.1.5. Activity assay of O-methyltransferase.....	16
2.1.6. HPLC Analysis	167
2.2.2 Virtual Screening.....	178

2.2.2. plasmid construction 오류! 책갈피가 정의되어 있지
않습니다.8

3. RESULTS.....	19
3.1.1 Identifying the key residues in EGCG binding pocket of <i>b</i> OMT responsible for regiospecificity.....	179
3.1.2. Evolution of <i>b</i> OMT for the synthesis of 3“Me EGCG...	191
3.2.1. Virtual screening for discovering more active EGCG <i>o</i> - methyltransferase.....	26
3.2.2 Enzyme expression and purification.....	302
3.2.3 <i>O</i> -methyltransferase activity assay.....	33
4. CONCLUSION.....오류! 책갈피가 정의되어 있지 않습니다.	
5. REFERENCES	36

List of Figures

Figure 1. The homology model of bOMT.

Figure 2. Multiple sequence alignment of OMTs.

Figure 3. The activities of mutants analyzed by HPLC.

Figure 4. Docking simulation comparing F163W with WT.

Figure 5. The phylogenic tree of *bm*OMT group

Figure 6. The phylogenic tree of *b*OMT group

Figure 7. The docking simulation results of candidate enzyme and EGCG

Figure 8. Sequence alignment of representative and identified sequence

Figure 9. SDS-PAGE gel of *bs*OMT, *ta*OMT, *pc*OMT, *hv*OMT

Figure 10. Specific methylation activities of 6 OMTs.

Figure 11. The kinetic parameters of *b*OMT, *bs*OMT, *ta*OMT.

List of Tables

Table 1. List of plasmids used in this study.

Table 2. List of plasmids constructed or used in this study.

1. Introduction

Tea is the one of the most famous traditional beverages in the world [1]. (-)-Epigallocatechin-3-*O*-gallate (EGCG) is the major polyphenol component of tea catechins. It is also the main active ingredient and shows various physiological and therapeutic effects, including anti-inflammatory and anti-allergy[2, 3], anti-bacterial and anti-viral[4, 5], anti-aging[6], cardiovascular disease[7]. Recently, the anti-fibro effect for lung against to COVID-19 was reported[8]. The fact of the efficacy relieving the lung fibrosis makes EGCG be the more attractive item in the nutraceutical market.

However, EGCG is very unstable in the blood and intestinal tract. It is easy to be auto-oxidation and degraded by the intestinal microbiome. Due to these traits, EGCG has low bioavailability on oral administration [9]. To enhance its pharmacokinetics, we choose the methyl modification which can induce the physicochemical change of EGCG. Especially, the D-ring of the EGCG has the main effect on its pharmacokinetics through oral administration. In fact, the bioavailability of (-)-epigallocatechin-3-*O*-(3-*O*-methyl)-gallate (3'' Me EGCG) was 2.7-fold higher than that of EGCG [10]. Furthermore, 3''Me EGCG has more active effect against on high-blood pressure and periodontitis as drugs[7, 11]. The site-specific methylation is the effective method for improving the efficacy of tea polyphenols.

The methylated EGCG rarely exists in nature tea extract (> 1 % w/w)[12]. the extraction of methylated EGCG from tea can't meet the industrial needs. The alternative ways to obtain 3''Me EGCG are chemical and enzymatic synthesis. However, the chemical synthesis needs the protection for hydroxyl group by using 2-nitrobenzenesulfonyl(Ns) protecting groups[13]. And then perform the deprotection reactions to remove protection group. These multiple extra reactions should need many reaction resources and time. Therefore, we thought that the enzymatic synthesis is the best way to produce the site-specific methylated EGCG for large scale.

The *S*-adenosyl-L-methionine dependent *o*-methyltransferase (SAM-dependent OMT) is the enzyme which can transfer the methyl group from SAM to the hydroxyl group by Sn2-like mechanism[14]. In the previous reports, several *o*-methyltransferases, which is isolated from *camelia sinensis* (tea) and *flammulina velutipes* (edible mushroom), were reported[15, 16]. They have activity for EGCG methylation. However, they had no regiospecific activity for 3'' Me EGCG. Therefore, we tried to find out the regiospecific OMT for 3''Me EGCG. Previously, our lab confirmed the bacterial enzymes from *bacillus megaterium* and *bacillus licheniformis*. The *bm*OMT was more active than *bl*OMT. In the contrast, the regioselectivity of *bm*OMT is lower than that of *bl*OMT.

In this study, we conducted the enzyme engineering to improve the activity of relatively regioselective *bl*OMT. we confirmed the two amino acid residues in active site that might play a key role in the

substrate binding and regioselectivity by docking simulation and alanine scanning. And then carried out the site directed mutagenesis by the rational design.

We also tried to discover the more active for EGCG methylation. To designate the candidate enzymes, we conducted bioinformatics analysis and docking simulation. Based on the *b*OMT sequence, we found out the more active bacterial OMT which can catalyze site-specific EGCG methylation.

2. Materials and methods

2.1.1. Chemicals and materials

EGCG, SAM-HCl were purchased from Sigma-Aldrich. Ethyl acetate was purchased from Junsei (Tokyo, Japan). LB Broth was purchased from BD dicfo. Oligomers were purchased from Bionics (Seoul, South Korea) and sequencing were purchased from Macrogen (Seoul, South Korea). Enzymes involved in restriction reaction, ligation were purchased from Thermo Scientific, TAKARA, respectively.

2.1.2. Sequence alignments and Docking simulation

Sequences of the *o*-methyltransferases were searched with PSI-BLAST in NCBI. To exclude redundant sequences, sequence clustering with the identity threshold of 90% was conducted by using CD-HIT. The 24 sequences were gathered and we used Clustal Omega to generation multiple sequence alignments[17].

The simulation for protein-ligand docking was conducted by AutoDock Vina. The pose with proper geometry for 3' hydroxyl group methylation and minimum binding energy was selected.

2.1.3. Site directed mutagenesis

The selected residues from multiple sequence alignment and docking simulation were mutated by using PCR. The plasmid vector containing *b*OMT sequence was used as a template. And then the proper primers were designed and applied for mutagenesis. The list of primers used in this study is in table 1.

2.1.4. Expression and purification of the enzymes

For the enzyme expression, the *o*-methyltransferase vector was transformed into *E. coli* BL21 (DE3) by using standard heat shock method. the colony was picked out from LB agar plate and cultured in 2 ml of LB broth with desired antibiotics under 37 °C overnight with shaking speed 200 rpm. 0.5 ml of cultured inoculum was added to 50 ml of LB and incubated at 37 °C until the OD₆₀₀ reached around 0.8~1.0. The Isopropyl-β-D-1-thiogalactopyranoside (IPTG) induction was performed in the concentration of 0.1 mM and the cells were incubated at 18 °C, 200 rpm for 16~18 hrs. After the induction, the cell was harvested and washed with 1X phosphate-buffered saline (pH 7.4) and resuspended in 5 ml of 50 mM Tris-HCl buffer (pH 8.0). the cell suspension was sonicated and centrifuged. The his-tagged OMT in supernatant was purified by using Ni-

NTA agarose bead (QIAGEN Korea Ltd., Seoul, Korea). The wash buffer (50 mM Tris-HCl, pH 8.0, 300 mM NaCl, 20 mM imidazole, 0.05 % tween 20) and elution buffer (50 mM Tris-HCl, pH 8.0, 300 mM NaCl, 250 mM imidazole) were used. The eluted enzyme solution was dialyzed by ultrafiltration for the removal of imidazole. The expression of enzymes was confirmed by SDS-PAGE gel analysis and the concentration of proteins was measured by Bradford assay.

BIOMT_F163A_F	GCAAAGGCCTTGTCGCATC
BIOMT_F163W_F	TGGAAAGGCCTTGTCGCATC
BIOMT_F163Y_F	TATAAAGGCCTTGTCGCATC
BIOMT_F163L_F	ATTAAAGGCCTTGTCGCATC
BIOMT_F163A_R	AAGGACATTGTCCGTAAAAATGATG
BIOMT_K164A_F	GCAGGCCTTGTCGCATCAG
BIOMT_F164A_R	GAAAAGGACATTGTCCGTAAAAATG

Table 1. List of plasmids used in this study.

	Origin	Antibiotics	Description	Reference
pET-24a(+)	pBR322	Km	pET-ma24 with OMT from <i>bacillus licheniformis</i>	In this study
pET-24a(+)	pBR322	Km	pET-ma24 with OMT from <i>bacillus megaterium</i>	In this study
pET-28(+)	pBR322	Km	pET-28 (+) with OMT from <i>paenibacillus chonroitinus</i>	In this study
pET-28(+)	pBR322	Km	pET-28 (+) with OMT from <i>heyndrickxia vini</i>	In this study
pET-28(+)	pBR322	Km	pET-28 (+) with OMT from <i>bacillus subtilis</i>	In this study
pET-28(+)	pBR322	Km	pET-28 (+) with OMT from <i>thermolongibacillus altinsuensis</i>	In this study

Table 2. List of plasmids constructed or used in this study.

2.1.5. Activity assay of *O*-methyltransferase

The 400 μ l reaction mixture containing 50 mM Tris-HCl (pH 8.0), 1 mM MgCl₂, 0.4 mM L-ascorbic acid(LAA), 0.2 mM EGCG, 0.4 mM SAM, 10 μ M OMT. The reaction mixture was incubated with shaking speed 200 rpm for 1h at 30 °C and the reaction was totally stopped by adding 80 μ l of 2 N HCl solution. methylated products were extracted by adding 850 μ l ethyl acetate to 150 μ l of the reaction mixture. After vigorous mixing and centrifugation, 800 μ l of the organic phase was collected and vacuum evaporated. The final sample was dissolved with 60 μ l of HPLC-grade methanol with 0.1 mM caffeic acid as internal standard and then analyzed with HPLC.

To determine kinetic parameters, the methylation reaction was conducted by varying the concentrations of the EGCG (0.025 mM ~ 0.4

mM). Except for the substrate concentration, other conditions were the same with those mentioned above. V_{\max} and K_m were calculated by non-linear regression based on Michaelis-Meten equation.

2.1.6. HPLC Analysis

The products were analyzed by HPLC(YL9100 HPLC, YoungLin, Korea) equipped with the phenomenex Luna[®] C18(2) column (5 μ m particle size, 100 Å, 150 x 4.6 mm) and UV detector. The mobile phase was (A) acetonitrile with 0.1 % trifluoroacetic acid (TFA) and (B) water with 0.1 % TFA. the gradient method was started at 15 % B mobile phase, followed by a linear increase from 15 % to 27 % for 15 min and then additional increase to 40 % for 3 min. The flow rate was 0.6 ml/min and detection UV range was 280 nm. The methylated product peaks were previously confirmed by ESI-TSQ, NMR [18].

2.2.1. Virtual Screening

The sequence set of *o*-methyltransferases was collected by using *blOMT* and *bmOMT* as query sequence from BLAST at RefSeq database in NCBI. And then the top 100 sequences were gathered for the subgrouping analysis. In each case of *blOMT* and *bmOMT*, a total of 101 sequences composed of 1 query sequence and 100 sequence collected by BLAST used for subgrouping by Subgrouping Automata (SA) algorithm

[19]. The homology modeling was carried out by using the representative sequences from SA. The possibility of the representative enzyme's activity for EGCG methylation was estimated by docking simulation.

2.2.2 Plasmid construction

The sequences of candidate protein were synthesized by LNC bio(Korea). The codon optimization was conducted for soluble expression of the enzymes. It was reported that rare codons in N-terminal sequences showed the effect on increasing the expression level of proteins.[20] We adopted the rare codon array to DNA sequence expressing 11 amino acids in the N-terminal region. The DNA sequence and pET-28(+) vector were cut by NcoI and XhoI restriction enzyme and then ligated.

3. Results and Discussion

3.1.1 Identifying putative EGCG and SAM binding site in *bOMT*.

The bacterial enzyme was isolated from *bacillus licheniformis* and had regioselective methylation activity for EGCG. Therefore, we decided to improve the activity of *b*OMT. To obtain the more detailed prediction of the substrate binding pocket of *b*OMT, the 3D structure of *b*OMT was modeled by using SWISS-MODEL based on the tRNA 5-hydroxyuridine methyltransferase (trmR) from *bacillus subtilis* (Identity: 66.8 %, PDB :5ZW3).[21]

SAM dependent *o*-methyltransferases which use SAM as methyl donor are well studied. It was reported that the residues which interact with SAM in the binding site are highly conserved [14, 22]. We tried to predict the putative EGCG binding pocket based on the methyl-transfer mechanism and conserved catalytic residues. Through the multiple sequence alignments (MSA) and Homology modelling, we confirmed the catalytic residue Lys136, and Mg²⁺ interaction residues Asp133, Asp159, Asn160 (fig. 1). And then we carried out the docking simulation to the pocket located near Mg²⁺ ion and the opposite site against SAM by using the AutoDock Vina[23].

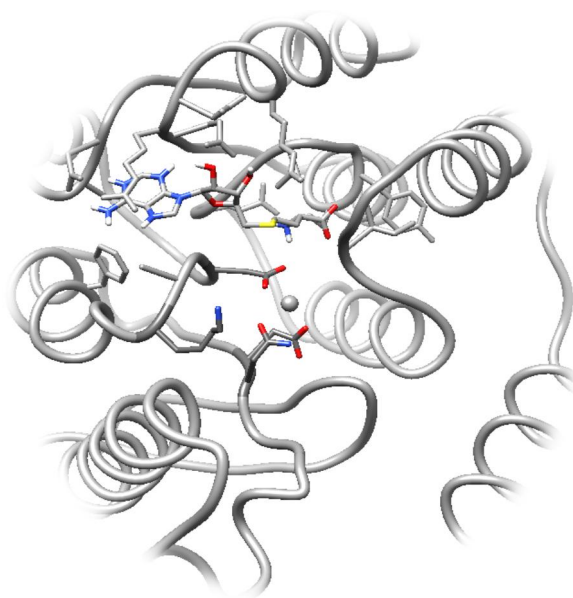


Figure 1. Homology model of *bOMT*. The catalytic residues in active site were colored.

3.1.2. Evolution of *bOMT* for synthesis of 3'Me EGCG

To enhance the activity and regioselectivity of *b*OMT for 3'-O-methylation of EGCG, we should choose the hot spot region which has effect on the enzyme reaction. The residues within 5 Å of substrate atoms were potential mutation sites for beneficial enzyme engineering [24]. The docking simulation of EGCG into putative binding site indicated that six residues (I37, M38, E39, D208, F163, K164) were selected within 5 Å from substrate atoms. Among these residues, three residues (I37, M38, E39) that the backbone of these amino acid seemed to interact with EGCG atoms were excluded from the list of mutation candidates. And D208 was also excluded because it is a highly conserved residue and known for interacting with hydroxyl group of the catechol substrate[25]. In this case, Asp may form the hydrogen bonding with hydroxyl group of the gallate moiety. The remaining residues (F163, K164) constitute the insertion loop which is located between α -helix 8 and β -strand 5. Previously, several reports indicated that the insertion loops near the active site have effect on the enzyme activity and substrate binding[26, 27]. From the multiple sequence alignments (fig. 2), the amino acid sequences of this region have low sequence homology, not conserved. Therefore, two residues (F163, K164) were chosen for assessing its effect on enzyme activity by conducting alanine substitution.

The F163A mutant showed the change of its regioselectivity for EGCG methylation. The peak representing 3'-Me EGCG from HPLC analysis was slightly separated. And the K164A mutant completely lost the activity of EGCG methylation. The HPLC analysis results of the

mutants (fig. 3A) suggested that Phe163 and Lys164 play a key role in determining the direction of the methylation and substrate binding.

The facts that the substitution of residues in insertion loop to aromatic or hydrophobic bulky amino acid showed the effect on enhancing the activity and regioselectivity were reported[28-30]. Therefore, we constructed the mutants, F163L, F163Y, F163W, and then confirmed their activity (fig. 3B). Among them, the F163W mutant showed about 2-fold initial reaction rate. F163Y decreased the initial rate and F163L completely lost its activity.

We assumed that the substitution to Trp might change the geometry of substrate binding to proper 3'-OH methylation. EGCG was docked into F163W mutant and compared with WT (fig. 4). The distance between the oxygen atom of the hydroxyl group and the carbon atom of the methyl group was shortened in F163W simulation.


```

4YMG EFDLIFVDANKDGYAGYVKTILDQGLLSANGIILCDNVFAR GLTIQPDCAFWLNDHVRPYWNGCGQALDKFSAGLMEDPRIDVLLLFV----FDGVTQIR
3NTV -YDMIFIDAARQAQSKKFF--EITYPLLKHQGLVITDNLVLYH GFVSD-IGIV----RSRNVRQMVKVQDYNEWLIKPGYTTNFLNI----DDGLAISI
2GPFY -FDVLFIDAARQQYRRFF--DMYSPMVRPGLLSDNVLFER GLVAET--DI----EHKRHKQLATKIDTYNQWLEHPQYDTRIFPV----GDGIAISI
5ZW3 -YDVFIDAARQQYQNFF--HLYEPLSPDGVIITDNLVLEK GLVAEDYSKI----EPKRRRLVAKIDEYNHWMNHPDYQTAIIPV----GGGLAISK
11ch1 -YDALFIDAARQQYQKFF--SIYEKMLADGGIIFTDNLVLEK GLVASEYNQI----ESKRKKLVSKIDHYNHWMLEHPDYHTAILFV----GGGLAVSQ
3C3F DIDILFMDCCDFVNGADVLE--ERMNRCLAKNALLIAVNALRR GSVAESHE-----D----PETAALREFNHHLRRRRDFTTIVFV----GNGVLLGY
3A7E TLDMVFLDHWKDRYLPDITLLEECGLLRKGTVLLADNVICP GAPDFLAH-----VRGSSCFECTHYQS---FLEYREV----VDGLEKAI
6AW4 TLDLVFLDHWKDRYLPDITLLEECGLLRKGTVLLADNVICP GTPDFLAY-----VRGSSCFECTHYSS---YLEYMKV----VDGLEKAV
4OAS -FDMI FIDANKSSYLAYL--NWAQMYIRKGGGLIVADNIFLE GSVFDEHP-----TEKVSSNAHASMRAFNDLANKEKYLSTIIPT----SEGMMVSI
6JCL -FDLVFIDADKENVVAYI--QWAIRLARRGAVIVVDNVIRG GGILAES--D----D----ADAVAARRTLQMMGEHPGLDATAIQTVGRKGDGFALAL
SNSD -FDMVFDANKPDIPEYF--TWALKLSRPGAVVVVDNVVLEK GAVTDPDH-P----D----AGVQGVRRFHEMLAGRSVDTATSITVGRKGYDGFLLAL
7CVX -FDMI FIDADKPPYTEYF--QWALRLSRPGTLIVADNVIRD GKVL DENS-T----E----PAVQGARRFNAMLGANTAVDATILQMVGVKEYDGMALAI
3TFW -FDLIFIDADKPNPHYL--RWALRYSRPGTLIIGENVVRD GEVVPQS-A----D----ERVQGVRFIEMMGAEPRLTATALQTVGRKGDGFLLAN
3DUL -FDFIFIDADKQNNPAYF--EWALKLSRPGTVIIGENVVRE GEVIDNTS-N----D----PRVQGIRRFYELIAAEPRVSATALQTVGSRKGYDGFIMAV
mega1 -FDLIFIDADKPNPNYL--KWALELSKRGSLIICDNVVRO GHVNSE-S-K----D----ENVKIRQFMNALLAQEKRI SATALQTVGSRKGYDGFIVGV
3C3Y SYDFGFVDADKPNYIKYH--ERLMLKLVKGGIVAYDNTLWG GTVAQPE-SE----VPDFMKENREAVIELNKL LAADPRIEIVHLPL----GGGITFCR
1SUI SYDFIFVDADKDNLYNH--KRLIDLKLVKGGVIGYDNTLWN GSVVAPPDAP----LRKYVRYRDFVLELNKALAVDPRIEICMLFV----GGGITICR
5KVA SFDFVFDADKDNLYNH--DRLLKLVKGGGLIGYDNTLWN GSVVLPDDAP----MRKYIRFYRDFVLVNLKALADERVEICQLFV----GGGVTLCR
5LHM TFDLAFIDADKESYDFY--EHALRLVRPGLLIIDNTLWS GKVADPSPVG----D----PETDSLRRINAKLLTDERVDSLMLPI----ADGLTLAR
2HNK SIDLFFLDADKENYPNY--PLILKLLKGGGLIADNVLWD GSVADLSH-Q----E----PSTVGIKRFNELVYNDSLVDVSLVPI----ADGVSLVR
2AVD TFDVAVVDADKENC S AYY--ERCLQLLRPGGILAVLRVLR GKVLQPPK-G----D----VAACEVRNLNERIRRDVRYISLLPL----GGGLTLAF
3CBG EFDLIFIDADKRNYPRY--EIGNLRLRRGGMLVIDNVLWH GKVTEVDF-Q----E----AQTQVLQQFNRLDQAQDERVRSVIFL----GGGMTLAF
3R3H QDFDFIDADKTNLYNH--ELALKLVTPKGLIADNIFWD GKVIDPND-T----S----GQTR EIKKLNQVKNDSRVFVSLLA I----ADGMFLVQ
-----

```

Figure 2. Multiple sequence alignment of OMTs. The box with gray color is the key residues for methylation. D133, D160, N161 hold Mg^{2+} ion. K136 removes the hydrogen of gallate moiety. D208 forms hydrogen bond with hydroxyl group.

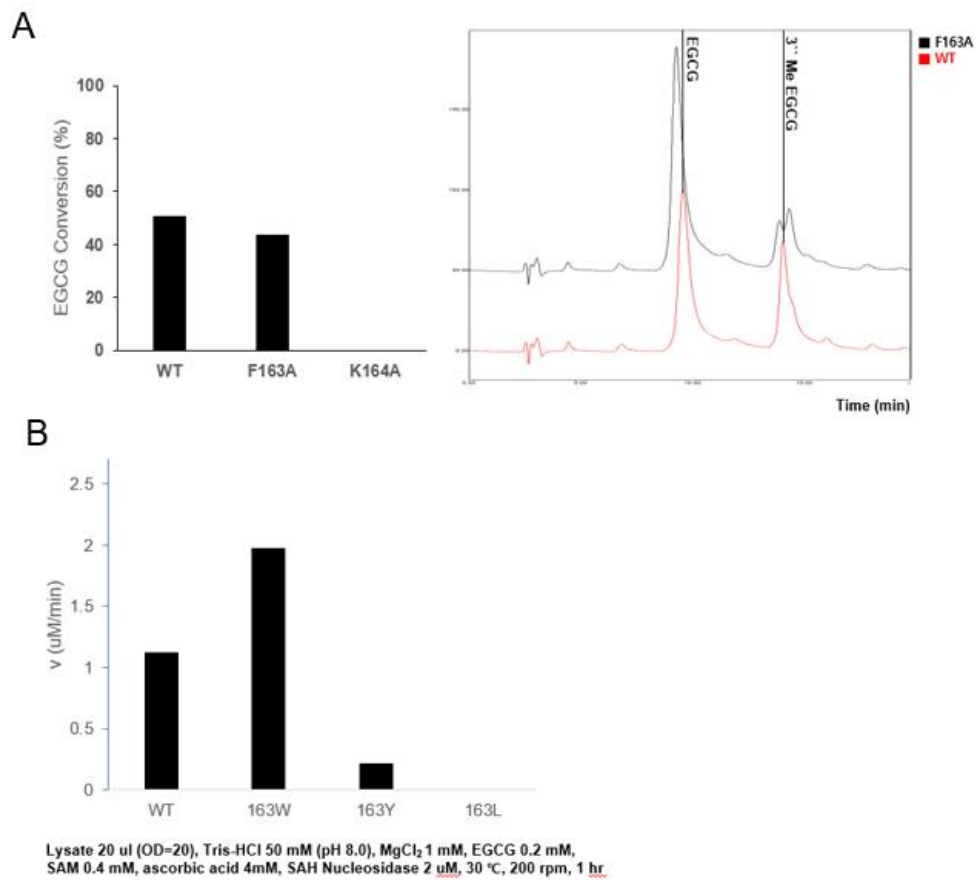


Figure 3. The activities of mutants analyzed by HPLC. (A) Alanine substitution mutant substrate conversion and HPLC chromatogram. (B) the reaction rate comparison of mutants (F163W, F163Y, F163L) with WT.

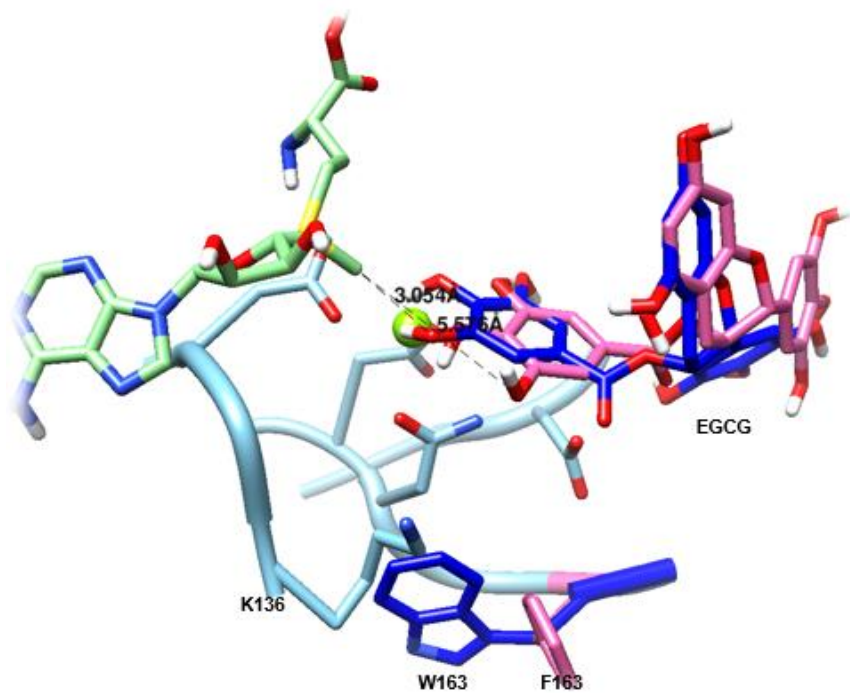


Figure 4. Docking simulation comparing F163W with WT. the distances between C atom of SAM and O atom of gallate were indicated. The EGCG with blue color is docked to F163W mutant. and pink one is docked to WT.

3.2.1. Virtual screening for discovering more active EGCG *o*-methyltransferase

To find out the more active *o*-methyltransferase, we carried out virtual screening which is combination of the method based on sequence and structure analysis. First of all, we gathered 2 sequence data sets from bLOMT and bmOMT each and conducted phylogenetic analysis (fig. 5, 6). To evaluate the average similarity of sequences in each subgroup, pairwise similarity was assessed by using multiple sequence alignments. The node which showed the drastic increase of average similarity was selected as the optimum node. As a result, input sets of bLOMT and bmOMT have two subgroups each. To select the representative sequence in the subgroup, we found out the most consensus sequence by using self-scoring method in Subgrouping Automata. Finally, the 4 OMTs from *thermolongibacillus altinseunsis* (taOMT), *bacillus subtilis* (bsOMT), *paenibacillus chondroitinus* (pcOMT), *heyndrickxia vini* (hvOMT) were selected as candidates to examine the activity for EGCG. To estimate whether to have the methylation activity for EGCG, homology modeling and docking simulation were conducted (fig. 7). From the docking simulation, we assumed that the 4 enzymes might produce the 3''Me EGCG and show higher activity because the distant between the sulfur atom of SAM and hydroxyl group of EGCG was shorter. To compare the residues which were predicted to interact with EGCG atoms, candidates

were aligned by clustal omega (fig. 8). It was confirmed that the sequences of the region interact with substrate are not identical.

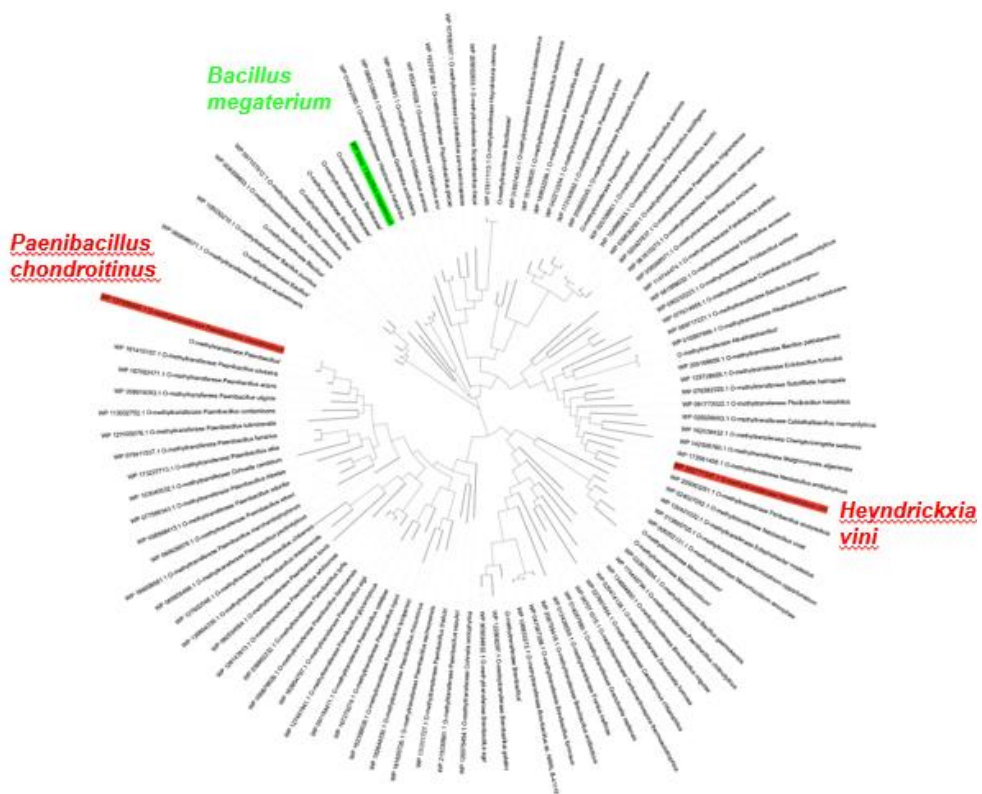


Figure 5. The phylogenetic tree of *bmOMT* group. the total of 101 sequences contained *bmOMT* was found by using BLAST at Refseq. The

representative enzymes from *paenibacillus chondroitinus* and *heyndrickxia vini* were chosen by Subgrouping Automata.

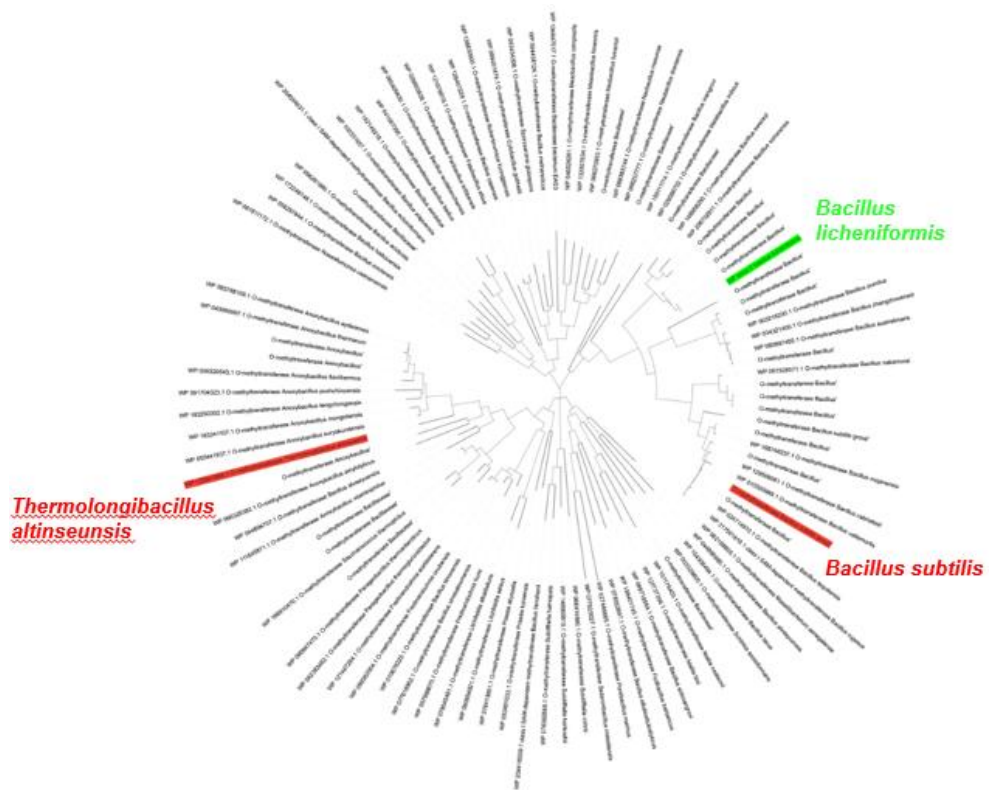
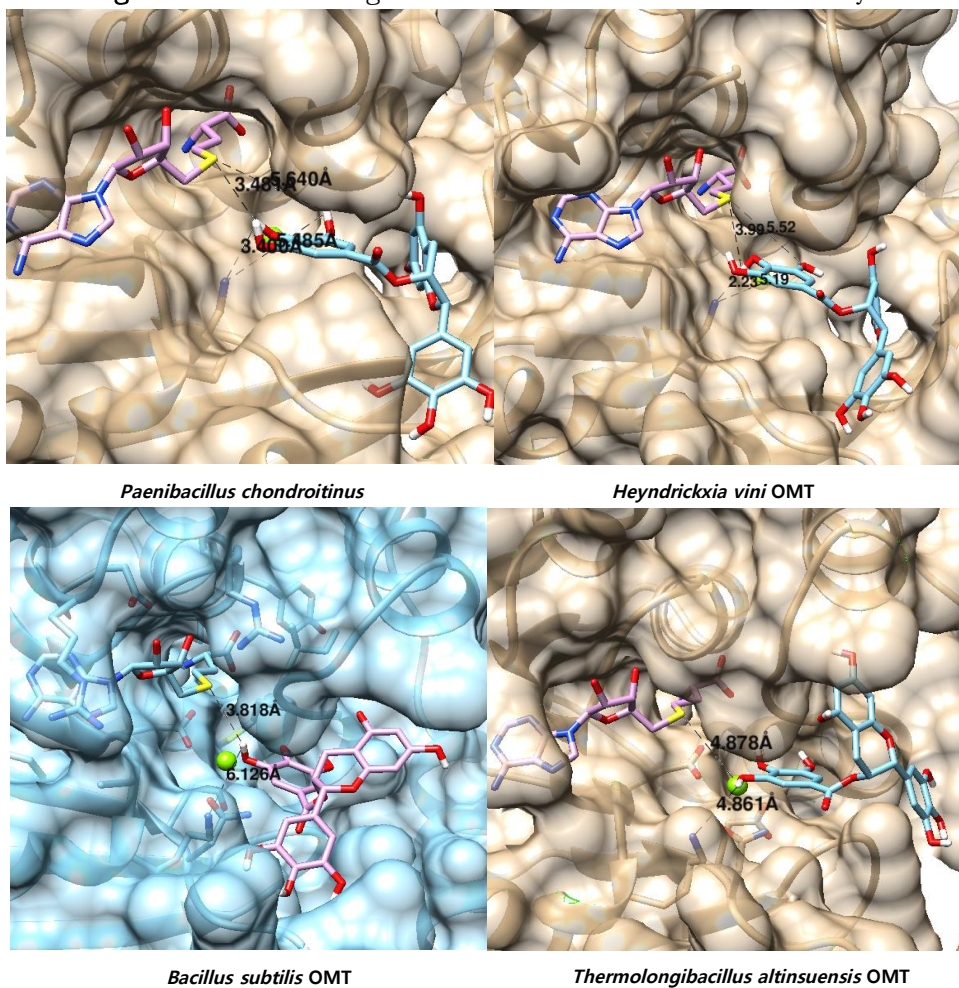


Figure 6. The phylogenetic tree of *bOMT* group. the total of 101 sequences contained *bOMT* was found by using BLAST at Refseq.

representative enzymes from *thermolongibacillus altinseunsis* and *bacillus subtilis* were chosen by Subgrouping Automata

Figure 7. The docking simulation results of candidate enzyme and



EGCG. the distances between hydroxyl group and methyl group were calculated.

```

pcOMT -MNA T N T W E K V D Q Y I K E R L I P H D T V L E N S L A A N Q L A G L P A Y D V S P T Q G K F L N L L I Q M K G A
hvOMT M G S I Y E I W N E V D L Y M N D K L I Q P D P I L D E V L K A N Q E A E L P A I D V S P S Q G K F L H L L A S L K G A
taOMT - M T K S E K W N E V D L Y F T S K L H A S D P Y M D S I L K A N A E A N L P A I D V S P N Q G K L L H L L A K L K G A
blOMT --- M Y N K E I V E Y I Q S L L P E R E E A I L K M E D Y A R E H H V P I M D L -- V G I E T M L H L L K I A N P
bsOMT --- M K I G H E E L T G Y L E K L L K P R P A E I M K L E A Y A E E H G V P I M E P -- T G I E Y L L Q L L S F K N P
                                     : : : * : * : : : : : : : : : : : : : : : : : : : : : : : : : : : : : : : : : : : : : : :

```



```

pcOMT K R I L E I G T L G G Y S T I W M A R A L P P D G K L Y T L E L D P I H A R V A S E N I S H A Q L S E L V E L R V G D A
hvOMT K R I L E I G T L G G Y S T I W L A R A L P K D G Q L I T L E L S A Q H A E V A R A N L K R A G Y S H L V E V I V G P G
taOMT K N I L E I G T L G G Y S S Y W L G R A L P E D G R L I T L E Y E Q K H A K V A E E N I R T A G L E N K I E V I V G P A
blOMT K K I L E I G T A I G Y S A I R M A K V L P N - A K I V T I E R D E E R Y K Q A L L Y V N E T K T S E Q I E V L F G D A
bsOMT K K I L E I G T A I G Y S A I R M A L A L P E - A E I F T I E R D E D R Y R E A L K N I R S F Q L E N R I H V F F G D A
                                     + . * * * * * * * * * : : . * * . . : : * + . : . * : . . . . : : : * .

```



```

pcOMT L E Q L A Q L D N E G V E P F D L I F I D A D K P N N P H Y L K W A L H F S H P G T V I I G D N V I R D G E V I N E E S
hvOMT L D T L A V L K D K G T D P F D L I F I D A D K P N N P N Y L K W A L E L S K R G S L I I C D N V V R Q G H V V N S E S
taOMT L E S L P T L K E R G F A N F D L I F I D A D K P N N P H Y L K W A L E Y S K P G T V I I G D N V V R R G R V I E E D S
blOMT L E L S D Q V A E -- K G P F D A L F I D A A K G Q Y R R F F E L Y E P L L T E R G I I I T D N V L F K G L V A S E Q -
bsOMT L S E S D P V Q S -- M A P Y D A L F I D A A K G Q Y Q K F F S I Y E K M L A D D G I I F T D N V L F K G L V A S E Y N
                                     * . : : : : * : * * * * * * : : : : : : : : : * : * * * * * * * * .

```



```

pcOMT Q D P R ----- V Q G Y R Q F Y D L L A D E P R I S A T A I Q T V G S K G Y D G F V L G I V K ----
hvOMT K D E N ----- V K G I R Q F M N A L A Q E K R I S A T A I Q T V G S K G Y D G F I V G V V E L E --
taOMT E D E S ----- I L G V R K F I D L L S K E P R I D S T A I Q T V G S K G Y D G F V L G I V K ----
blOMT P I E Q K R I R Q L V Q K I R E Y N E W L M N H P R Y E - T I I L P I G ---- D G M A I S R R R G E --
bsOMT Q I E S K R I K K L V S K I D H Y N H W L M E H P D Y H - T A I I P V G ---- D G L A V S Q K R G E R I
                                     K I E P K R R R R L I T K I D E Y N H W L M N H P D Y Q - T A I I P V G ---- D G L A I S K K K R ---
                                     : : : : : * . . . . * * * * * * * * * * * * * * : : : : :

```

Figure 8. Sequence alignment of representative and identified sequence (*blOMT*, *bmOMT*, *pcOMT*, *hvOMT*, *taOMT*, *bsOMT*). The box with colored indicate the residues located within 5 Å from docked EGCG atoms.

3.2.2. Enzyme expression and purification

The candidate enzymes selected by bioinformatics tools were completely cloned in *E. coli* BL21 (DE3). the heterologous expression and His-tag purification was confirmed by SDS-PAGE gels (fig. 9).

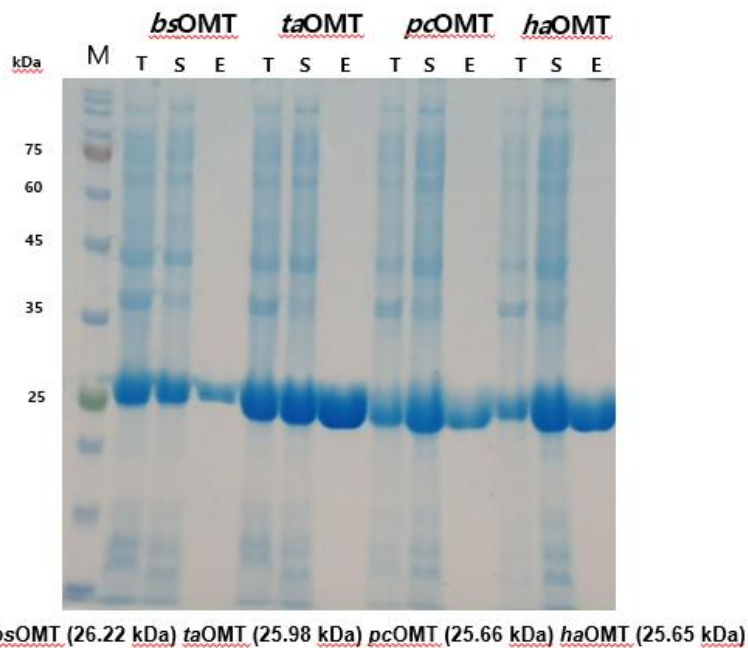


Figure 9. SDS-PAGE gel of *bsOMT*, *taOMT*, *pcOMT*, *hvOMT*.
M: marker, T : total fraction, S : soluble fraction, E : Elution.

3.2.3 *O*-methyltransferase activity assay

The methylation reaction was conducted by purified enzyme and analyzed by HPLC. The activities of the 4 enzymes were higher than *b*OMT and *bm*OMT. The reaction rates and product compositions were compared. (fig. 10). *hv*OMT and *pc*OMT showed reaction rates about 2-fold and 1.3-fold higher than *bm*OMT, respectively. *ta*OMT and *bs*OMT also showed reaction rates about 1.7-fold and 1.3-fold higher than *b*OMT. The new enzymes had similar reaction tendencies to the identified enzymes. Among the candidate enzymes, *hv*OMT and *pc*OMT showed better activities but still performed the additional methylation reaction, whereas *ta*OMT and *bs*OMT showed lower reaction rates but had higher regioselectivity for 3''Me EGCG. we thought the engineering of *ta*OMT and *bs*OMT to enhance the activity and maintain the regioselectivity is the better way. Therefore, we carried out the further kinetic assay for *ta*OMT and *bs*OMT. The kinetic parameters were calculated by nonlinear regression applied to Michaelis & Menten equation (fig. 11).

The structural differences between *b*OMT group and *bm*OMT group are the amino acid constitution in the insertion loop and the size of the active site pocket. The residues, Phe and Asp was reported that they have effect on gating elements which is important for substrate specificity. The change of the gating element to small amino acid enhanced the activity of enzyme but substrate selectivity was to be broad. [31] *b*OMT group containing *ta*OMT and *bs*OMT has the Phe residue in the insertion loop near active site, whereas *bm*OMT group has no bulky

amino acid. Therefore, bmOMT group could produce di-methylated EGCG and show the higher activity.

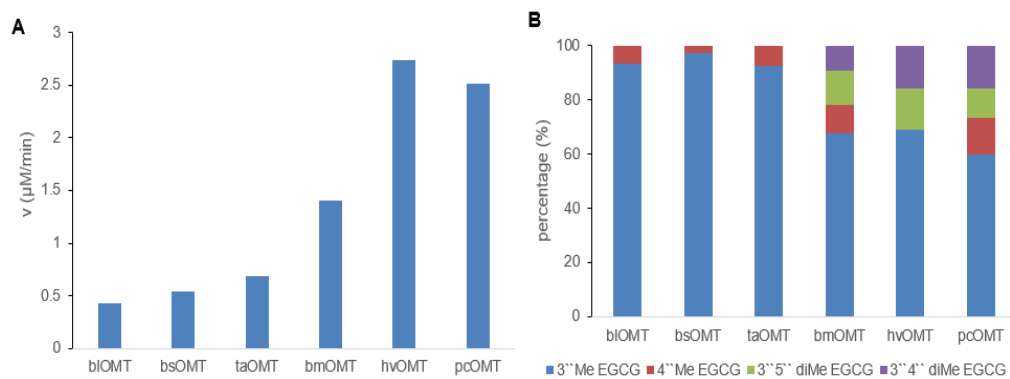
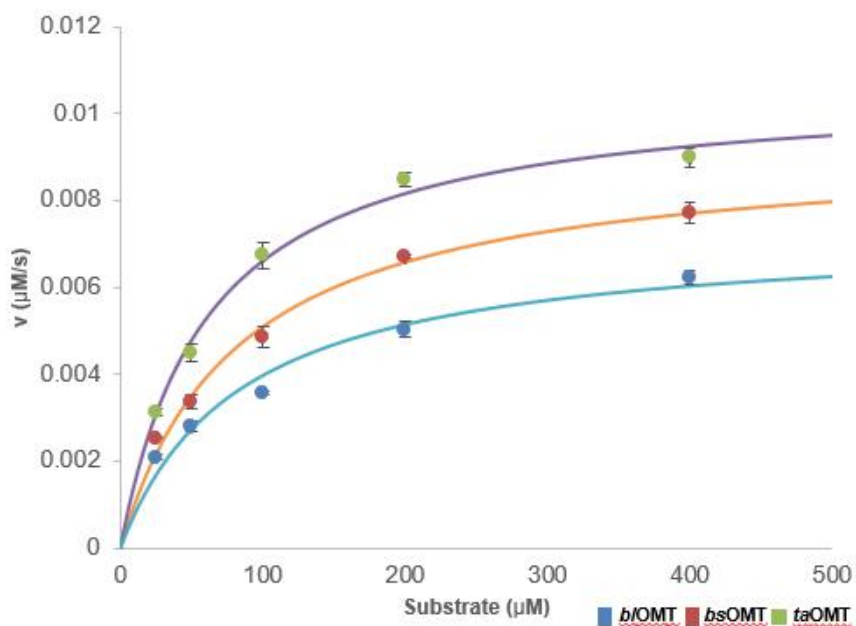


Figure 10. Specific methylation activities of 6 OMTs. (A) the initial rate of OMTs (B) the content of products by enzymatic reaction.



	K_m (μM)	k_{cat} (s^{-1})	k_{cat}/K_m ($\mu\text{M}^{-1}\text{s}^{-1}$)	Relative k_{cat}/K_m
<u>bIOMT</u>	83.6	0.00073	8.73	1
<u>bsOMT</u>	82.4	0.00093	11.29	1.3
<u>taOMT</u>	61.5	0.00107	17.41	2.0

Figure 11. The kinetic parameters of *bIOMT*, *bsOMT*, *taOMT*.

4. Conclusion

We confirmed that the insertion loop of the *b*OMT, especially 163, 164 residues, has the effect on binding of EGCG and regioselectivity. The mutation to hydrophobic aromatic ring amino acid enhanced the methylation activity and it can be adopted to other *o*-methyltransferase. We also found out the more active *o*-methyltransferases by using bioinformatics tools based on previous identified enzyme and confirmed their activity for EGCG site-specific methylation. These enzymes can be used for 3'-Me EGCG production or other methylated EGCG. In further studies, we will conduct the mutation to insertion loop of *ta*OMT and OMT and confirm the activity of mutants.

5. References

1. Pasrija, D. and C. Anandharamakrishnan, *Techniques for extraction of green tea polyphenols: a review*. Food and Bioprocess Technology, 2015. **8**(5): p. 935-950.
2. Fechtner, S., et al., *Molecular insights into the differences in anti-inflammatory activities of green tea catechins on IL-1 β signaling in rheumatoid arthritis synovial fibroblasts*. Toxicology and applied pharmacology, 2017. **329**: p. 112-120.
3. Maeda-Yamamoto, M., et al., *O-methylated catechins from tea leaves inhibit multiple protein kinases in mast cells*. The Journal of Immunology, 2004. **172**(7): p. 4486-4492.
4. Giri, K., et al., *Antibacterial effect of green tea extract against multi drug resistant Escherichia coli isolated from urine sample of patients visiting tertiary care hospital of Eastern Nepal*. International Journal of Applied Sciences and Biotechnology, 2020. **8**(1): p. 45-51.
5. Xu, J., et al., *Green tea extract and its major component epigallocatechin gallate inhibits hepatitis B virus in vitro*. Antiviral research, 2008. **78**(3): p. 242-249.
6. Chen, J., et al., *Anti-skin-aging effect of epigallocatechin gallate by regulating epidermal growth factor receptor pathway on aging mouse model induced by d-Galactose*. Mechanisms of Ageing and Development, 2017. **164**: p. 1-7.
7. Wolfram, S., *Effects of green tea and EGCG on cardiovascular and metabolic health*. Journal of the American College of Nutrition, 2007. **26**(4): p. 373S-388S.
8. Zhang, Z., et al., *Potential protective mechanisms of green tea polyphenol EGCG against COVID-19*. Trends in Food Science & Technology, 2021.
9. Dai, W., et al., *Bioavailability enhancement of EGCG by structural modification and nano-delivery: A review*. Journal of Functional Foods, 2020. **65**: p. 103732.

10. Oritani, Y., et al., *Comparison of (–)-epigallocatechin-3-O-gallate (EGCG) and O-methyl EGCG bioavailability in rats*. Biological and Pharmaceutical Bulletin, 2013. **36**(10): p. 1577-1582.
11. Tominari, T., et al., *Effects of O-methylated (–)-epigallocatechin gallate (EGCG) on LPS-induced osteoclastogenesis, bone resorption, and alveolar bone loss in mice*. FEBS open bio, 2017. **7**(12): p. 1972-1981.
12. Suzuki, T., et al., *Green tea extract containing a highly absorbent catechin prevents diet-induced lipid metabolism disorder*. Scientific reports, 2013. **3**(1): p. 1-7.
13. Asakawa, T., et al., *Syntheses of methylated catechins and theaflavins using 2-nitrobenzenesulfonyl group to protect and deactivate phenol*. The Journal of antibiotics, 2016. **69**(4): p. 299-312.
14. Tsao, D., L. Diatchenko, and N.V. Dokholyan, *Structural mechanism of S-adenosyl methionine binding to catechol O-methyltransferase*. PLoS One, 2011. **6**(8): p. e24287.
15. Kirita, M., et al., *Cloning of a novel O-methyltransferase from Camellia sinensis and synthesis of O-methylated EGCG and evaluation of their bioactivity*. Journal of agricultural and food chemistry, 2010. **58**(12): p. 7196-7201.
16. Kirita, M., et al., *Purification and characterization of a novel O-methyltransferase from Flammulina velutipes*. Bioscience, biotechnology, and biochemistry, 2014. **78**(5): p. 806-811.
17. Madeira, F., et al., *The EMBL-EBI search and sequence analysis tools APIs in 2019*. Nucleic acids research, 2019. **47**(W1): p. W636-W641.
18. 노희원, *Cloning and expression of small laccase Sv1 from Streptomyces viridosporus and its application to develop dyeing strain for wool fabrics and polyol chain extender for self-healable polyurethane*, in 방선균 유래의 락케이즈 Sv1 의 클로닝, 발현을 통한 양모 염색 균주의 개발 및 자가 치유가능 PU 생성을 위한 폴리올 사슬 연장체의 합성. 2020, 서울 : 서울대학교 대학원: 서울.

19. Seo, J.-H., et al., *Subgrouping Automata: Automatic sequence subgrouping using phylogenetic tree-based optimum subgrouping algorithm*. Computational biology and chemistry, 2014. **48**: p. 64-70.
20. Goodman, D.B., G.M. Church, and S. Kosuri, *Causes and effects of N-terminal codon bias in bacterial genes*. Science, 2013. **342**(6157): p. 475-479.
21. Waterhouse, A., et al., *SWISS-MODEL: homology modelling of protein structures and complexes*. Nucleic acids research, 2018. **46**(W1): p. W296-W303.
22. Sun, Q., M. Huang, and Y. Wei, *Diversity of the reaction mechanisms of SAM-dependent enzymes*. Acta Pharmaceutica Sinica B, 2021. **11**(3): p. 632-650.
23. Trott, O. and A.J. Olson, *AutoDock Vina: improving the speed and accuracy of docking with a new scoring function, efficient optimization, and multithreading*. Journal of computational chemistry, 2010. **31**(2): p. 455-461.
24. Paramesvaran, J., et al., *Distributions of enzyme residues yielding mutants with improved substrate specificities from two different directed evolution strategies*. Protein Engineering, Design & Selection, 2009. **22**(7): p. 401-411.
25. Lee, S., J. Kang, and J. Kim, *Structural and biochemical characterization of Rv0187, an O-methyltransferase from Mycobacterium tuberculosis*. Scientific reports, 2019. **9**(1): p. 1-12.
26. Kopycki, J.G., et al., *Biochemical and structural analysis of substrate promiscuity in plant Mg²⁺-dependent O-methyltransferases*. Journal of molecular biology, 2008. **378**(1): p. 154-164.
27. Walker, A.M., et al., *The structure and catalytic mechanism of Sorghum bicolor caffeoyl-CoA O-methyltransferase*. Plant Physiology, 2016. **172**(1): p. 78-92.

28. Cai, Y., et al., *Engineering a monolignol 4-O-methyltransferase with high selectivity for the condensed lignin precursor coniferyl alcohol*. Journal of Biological Chemistry, 2015. **290**(44): p. 26715-26724.
29. Yang, L., et al., *Biosynthesis of plant tetrahydroisoquinoline alkaloids through an imine reductase route*. Chemical science, 2020. **11**(2): p. 364-371.
30. Law, B.J., et al., *Effects of active-site modification and quaternary structure on the regioselectivity of catechol-O-methyltransferase*. Angewandte Chemie International Edition, 2016. **55**(8): p. 2683-2687.
31. Kingsley, L.J. and M.A. Lill, *Substrate tunnels in enzymes: structure–function relationships and computational methodology*. Proteins: Structure, Function, and Bioinformatics, 2015. **83**(4): p. 599-611.

국문 초록

에피갈로카테킨 갈레이트(EGCG)는 녹차 추출물의 대표적인 생리 활성 물질로 유망한 뉴트라슈티컬 물질이다. 다양한 생리적 및 약리적 효과로 건강기능식품이나 화장품 재료로 많이 사용된다. 하지만 에피갈로카테킨 갈레이트(EGCG)의 체내 환경에서의 불안정성과 낮은 막 투과율로 인해 생체이용율이 낮아 활용에 제한이 있다. 따라서 본 연구에서는 생체이용율이 높은 3'' 메틸 에피갈로카테킨 갈레이트의 효과적인 합성을 목적으로 위치특이적으로 메틸화 변형이 가능한 효소의 개량과 발굴에 관한 연구를 진행하였다.

이전 활성을 확인했던 *bacillus licheniformis*의 활성부위에서 기질 결합과 반응에 영향을 미치는 잔기를 확인하고 변이를 통해 반응속도가 2 개 증가한 변이주를 찾았다. 해당 부위는 다른 메틸전이효소에도 적용이 가능하다.

더 높은 활성을 가지는 효소를 찾기 위해 서열과 구조 기반의 생물정보학 분석을 통해 활성이 높을 것으로 예상되는 효소를 후보를 골라 활성을 시험했다. 결과적으로 *Thermolongibacillus altinsuensis*, *bacillus subtilis*, *paenibacillus chondroitinus*, *heyndrickia vini* 4 개 효소를 대장균에서 발현하고, 기준 효소보다 특이적인 메틸화 반응의 활성이 더 높은 것을 확인하였다. 이를 통해 'Subgrouping Automata'와 도킹 시뮬레이션을 통한 예측이 효과가 있음을 확인하였고, 하위 서브 그룹 시험을 통해 추가적인 효소 발굴이 적용할 수 있다는 점에 의의가 있다.

주요어: 에피갈로카테킨 갈레이트, 위치 선택성, 메틸전환효소,
서브그룹 오토마타

학번: 2020-28874